energies

MDPI

Article

Application of Near Infrared Spectroscopy for the Detection of Chemically Treated Pellets Unsuitable for Combustion

Elena Leoni [1], Thomas Gasperini [1], Nicolò Di Marzio [2], Rodolfo Picchio [3], Giuseppe Toscano [1] and Daniele Duca [1,*]

[1] Department of Agricultural, Food and Environmental Sciences, Polytechnic University of Marche, Via Brecce Bianche, 60131 Ancona, Italy; e.leoni@univpm.it (E.L.); t.gasperini@univpm.it (T.G.); g.toscano@univpm.it (G.T.)
[2] Department of Land, Environment, Agriculture and Forestry, University of Padua, Viale dell'Università, 35020 Legnaro, Italy; nicolo.dimarzio@studenti.unipd.it
[3] Department of Agricultural and Forest Sciences (DAFNE), Tuscia University, Via San Camillo de Lellis, 01100 Viterbo, Italy; r.picchio@unitus.it
* Correspondence: d.duca@univpm.it

Abstract: The relevant growth of the wood pellet market in Europe in the last decade led to an increased focus on solid biofuel as a necessary and available renewable resource for energy production. Among biofuels, wooden pellets are among the most widespread for domestic heating. Therefore, monitoring the qualitative properties of commercialized pellets is crucial in order to minimize the amount of harmful emissions in residential areas. Standard ISO 17225 sets threshold values for the chemical and physical properties that commercialized biofuels must fulfil. Specifically, ISO 17225-2 defines that pellets for residential use must be produced from virgin wood, but no method is proposed to assess the actual origin of the material, leading to the risk of the commercialization of pellets made up from chemically treated materials. This study proposes a model obtained via near infrared spectroscopy analyses and chemometrics methods, such as classification, to rapidly assess whether pellets are made up of virgin or chemically treated wood. The result suggests the effectiveness of NIRs for the detection of non-virgin pellets with an accuracy greater than 99%. Furthermore, the model appeared to be accurate in the assessment of both milled and intact pellets, making it a potential in-line instrument for assessments of pellets' quality.

Keywords: chemically treated pellets; NIRs; emissions; classification; PLS-DA; NOx

Citation: Leoni, E.; Gasperini, T.; Di Marzio, N.; Picchio, R.; Toscano, G.; Duca, D. Application of Near Infrared Spectroscopy for the Detection of Chemically Treated Pellets Unsuitable for Combustion. *Energies* **2024**, *17*, 825. https://doi.org/10.3390/en17040825

Academic Editor: Dariusz Kardaś

Received: 15 December 2023
Revised: 12 January 2024
Accepted: 7 February 2024
Published: 9 February 2024

1. Introduction

Over the last decade, there has been a noticeable growth in Europe's wood pellet market [1–3]. The growth is reflected by the increased production, which has reached an average of 18,178 thousand tons between 2020 and 2023, compared with the 2013–2019 average production of 14,960 thousand tons. Specifically, since 2013, the Italian pellet market has been characterized by an increase in production and imports by 13% and 10%, respectively [4].

Whilst European green policies have contributed to the shift towards renewable energies and the increased use of wood pellets [5], it is acknowledged that solid biofuels can contribute to the production of gaseous and particulate emissions [6–8]. For example, Bäfver et al. investigated the amount of particulates emitted by pellet stoves and residential wood stoves during combustion, recording up to 82 mg/MJ of particulate matter [9].

The quality of the emissions and flue gases is affected by the way in which the heating systems are used [10] (e.g., adjusting the combustion air inlets) and by the biofuel's quality [11–13]. In fact, a number of studies have highlighted the significant impact of wooden pellets' properties, such as length, moisture and bulk density, on the efficiency of combustion in pellet stoves [14–16], whilst Mack et al. assessed the potential negative

effects of organic additives used during pelletization on particulate emissions [17]. For this reason, the use of high-quality materials for producing pellets is of crucial importance. Therefore, as the biofuel market has developed, so has the focus on pellet quality. To this end, ISO standards have been introduced.

Standard ISO 17225-2 defines quality classes for pellets and the threshold values for the chemical, energetical and physical parameters [18]. The aforementioned standard states that commercialized wooden pellets for residential applications should originate exclusively from virgin wood or chemically untreated wood. Furthermore, given the effects that chemical and physical parameters have on the quality of emissions, the thresholds for the quality parameters have been set to be particularly restrictive (i.e., those for nitrogen and ash content).

However, in accordance with the principle of recycling and ennoblement of waste materials, a number of studies have investigated the use of chemically treated wood for producing pellets. Risholm-Sundman et al. and Jiang Jinrui et al. investigated and compared the quality of emissions during the combustion of wooden materials containing adhesives and untreated pellets, recording an increase in nitrogen oxide (NOx) emissions from the combustion of the former [19,20]. A number of studies have explored the possibility of reusing waste from the engineered wood industry, such as medium-density fiberboard (MDF) and oriented strand board (OSB) waste. These materials are composed of wood pulp mixed with adhesives or resins. MDF, for instance, is made by blending wood powder, which is then mixed and compacted with adhesives such as urea–formaldehyde (UF) [21]. However, adhesives such as UF are nitrogen-based polymers and therefore contribute to increased levels of NOx in flue gases when combusted [19,22].

Over the last few years, Italy implemented a policy which only allows the use of certified pellet-fueled domestic heating systems with extremely low NOx and particulate emissions [23,24]. Whilst emissions can be affected by the usage of heating systems, it is clear that monitoring the quality of the pellets used in these systems is crucial.

Laboratory analyses are an effective method to assess biofuels' quality; however, they are both costly and time-consuming. Therefore, innovative rapid systems are required to enable the detection of the features of pellets that are not suitable for domestic combustion. Among the innovative technologies used in the field of biomasses, spectroscopy is one of the most widely applied. Several studies have investigated the use of infrared spectroscopy (IR) to assess the overall quality of pellets [25–27]. However, the application of IR is not limited to biofuels; in fact, spectroscopy, combined with the application of chemometrics, is also broadly used in quality control for food [28,29]. So far, the application of near infrared (NIR) spectroscopy is regulated by the technical standard UNI/TS 11765-2019, which, however, acts only as a guideline. One of the most applied and studied chemometric methods paired with NIR are principal component analysis (PCA), partial least squares regression (PLS) and PLS discriminant analysis (PLS-DA) [30–32]. In particular, PCA and PLS-DA allow the investigation and classification of materials according to their chemical and, consequently, physical properties, enhancing the evaluation of their intrinsic compositional characteristics, thus becoming a support tool for the monitoring of biomasses' source materials [33–35]. For instance, Lixourgioti et al. applied chemometric methods to detect adulterations in commercialized cinnamon [36], whilst Dupuy et al. investigated the use of IR modelling to assess the quality of virgin olive oil [37]. Furthermore, the organoleptic properties of coffee can be controlled to enhance the quantification of adulterated matrices [38]. IR and PCA can also be used to investigate wood's quality traits by assessing the effects of physical characteristics on the discrimination of species. This approach offers the advantage of significant time and cost savings [39,40]. Additionally, softwoods and hardwoods can be distinguished by applying PCA based on the main chemical differences between the two macro-groups [41]. Classification models could provide a deep knowledge about the source origin and chemical components, promoting immediate and non-invasive investigations directly in field because they are easily implemented along the production and supply chain [27]. Within the field of biomasses, it can be implemented in heating systems,

allowing for a continuous monitoring of the efficiency of combustion [42]. PLS-DA has been successfully used by Nascimbem et al. to determine and classify wood chips' quality [43], and also to improve qualitative assessments of the separation between sapwood and heartwood according to evaluations of the density of the species [44]. A number of studies proposed using PLS-DA classification models to discriminate wood species, according to their similar chemical and physical features [45], but also to discriminate pure species and hybrids, providing higher quality control in breeding and plantation programs [46]. Moreover, the classification of solid biofuels according to their origin and species is a fundamental key to improving the performance of energy production, due to the different calorific values, improving the combustion control and the technical efficiency of heating systems [47].

Classification also aims to support the detection of the illegal use of waste materials, which can be difficult to identify in densified and homogenous products such as pellets. This helps to reduce the negative environmental impacts caused by the combustion of unsuitable materials [48,49]. Identification of both the treated components and the origin is crucial to ensure continuous and direct control of commercialized pellets and guarantee compliance with the environmental and safety requirements set by the standards [50].

Acknowledging the previous applications and the need to monitor the presence of treated material during pelletization, this study proposes the use of an NIR chemometrics method of PLS-DA to develop a classification model for laboratory-produced pellets. To classify virgin and treated wood pellets, woody materials were processed and tested at every production step, starting from the raw materials. This was carried out to assess whether and how the pelletization process could affect the chemical structure of the wood under different physical conditions. Furthermore, the use of a benchtop NIR spectrophotometer allowed the simulation of an in-line system, leading to a huge number of replicates and a more representative dataset. Therefore, the laboratory production of pellets using different virgin and treated materials allowed the evaluation of NIR's ability to identify illegal components, providing an intuitive and faster screening tool to prevent the trading and usage of unsuitable pellets.

2. Materials and Methods

The research was carried out in two stages. The former involved the gathering of virgin and chemically treated wood, followed by grinding and pelletization; the latter involved a spectroscopic analysis via NIR of the ground raw materials (with the code GR0), pellets (with the code IN) and the dust obtained by grinding the pellets (with the code GR1) in order to assess whether pelletization process might influence the spectral response of materials. The NIR data were processed to develop statistical models for the identification and classification of virgin untreated and chemically treated wood. Detailed descriptions of each step of the methodology are presented in the following sections.

2.1. Gathering of the Raw Materials

Both untreated (V) and chemically treated wood (T) residues were obtained from wood-processing companies across Italy during 2023, thus constituting 2 distinct groups of samples. T materials were primarily treated with UF adhesive. Both the V and T groups consisted of samples with at least 2 kg of material. The materials were cut and ground to a particle size of 5 mm using a SM300 cutting mill produced by Retsch (Düsseldorf, Germany). The different materials were separated and distinguished by the suppliers. As a result, 45 samples in total were obtained, specifically 14 from V and 31 from T (Table 1).

2.2. Pelletization of Samples

V and T samples were pelletized using a Ceccato pelletizer with nominal power of 4 kW and a maximum production capacity of 60–70 kg/h. The pelletizer was equipped with a 6 mm flat die model for the production of pellets with a length of 30 mm (±5 mm). Before production, the pelletizer was warmed up at an optimal temperature of 70 °C by pelletizing

fir wood that was not part of the samples. Once the optimum temperature was reached, indicated by the outflow of durable pellets, the residual fir wood was removed, then the production of samples started. The production cycle was monitored by maintaining a variable temperature range between 60 and 100 °C. The die was cleaned with compressed air between each sample, along with each tool used during production, thus avoiding contamination. In addition, at the start of production of each sample, the first part of the raw material was used to prime the pelletizer, discarding the first pellet produced, to ensure the purity of each sample. Furthermore, additional moistening was carried out to the raw materials, ensuring a better pelletization process. In total, 2 kg of pellets was produced for each sample.

Table 1. Type and number of samples analyzed.

Origin	Type	No. of Samples
T	Multilayer board	9
T	Block board	4
T	Medium-density fiberboard	3
T	Particle board	11
T	Oriented strand board	4
V	Coniferous virgin wood	1
V	Fir wood	11
V	Beech wood	1
V	Oak wood	1

T: chemically treated wood; V: virgin or untreated wood.

2.3. NIR Analysis

NIR analysis was performed using a NIRMaster^{TM} instrument distributed by Buchi Italia S.r.l. (Cornaredo, Italy). The spectrophotometer, abbreviated as Buchi, works in the range between 800 and 2500 nm, and it is equipped with twin tungsten halogen lamps as the source and an extended-range indium gallium arsenide (InGaAs) photodiode array detector. The benchtop spectrophotometer (weighing about 40 kg) is provided in a compact case, in which the illumination spot, 9 mm in diameter, is placed in the upper part and covered by an unbreakable cup of hardened glass that spins around the spot for a minimum time of 4 to a maximum of 16 s for each replicate, collecting 2–4 scans/s. The sample-placing plate, which has a circular motion, must be adequately filled with the sample material to avoid the interference of external light and the occurrence of scattering effects. The plate (with a diameter of 10 cm) allows for the analysis of a substantial amount of material, improving the representativeness of the data. The circular motion simulates in-line acquisition, facilitating the collection of a large number of scans and reducing errors in the analysis. The acquisition was performed in reflectance mode, with both internal (gold plate) and external (Spectralon) reference measurements acquired at the start and every hour of analysis. The analysis was conducted at each stage (GR0, IN and GR1) and repeated nine times after proper mixing of the sample. The final dataset consisted of 45 samples for 9 replicates each, thus there were 405 spectra $\times$ 1501 variables.

2.4. Data Processing

Various chemometric methods were applied to examine the spectral dataset prior to class modelling. Several spectral pretreatments have been developed to enhance the information responsible for the classification of samples and to remove the noise mainly caused by the scattering effect. Specifically, scatter-correction pretreatment techniques such as SNV (standard normal variate) and MSC (multiplicative scatter correction) were considered, as well as derivative techniques (first- and second-order with a Savitzky–Golay filter and using different window points) [51,52].

PCA was carried out to assess the visual separation between V and T, and it was performed on mean-centered data. Specifically, the graphical visualization of the samples' separation and the assignment of the influence of chemical components were shown in

the score plot and loading plot of the best pretreated model. Subsequently, PLS-DA was performed as the classification method, which was based on the relationship between the spectral data and the dependent variable, namely, a binary dummy variable that specified whether the sample belonged (value 1) or did not belong (value 0) to a specific group [43,44]. A confusion matrix (Table 2) was developed to assess the number of correctly and incorrectly classified samples. The sum of correctly classified samples is expressed as TP (true positive) and TN (true negative) samples, whilst the sum of FN (false negatives) and FP (false positives) represent the incorrectly classified fraction. The plot of sensitivity (true positive rate or TPR) versus 1-specificity (false positive rate or FPR) was used to construct the receiver operating characteristics (ROC) curve, where the area under the curve showed the accuracy of classification, and thus the model's ability to discriminate between two different classes. Accuracy was also calculated as the sum of TN and TP samples (correctly classified samples) divided by the total of the dataset. The ROC curve's value was considered as the threshold of decision, so when ROC = 0.5, the model was not able to divide the samples into classes and only random separation occurred. The closer the curve was to the upper lefthand corner in the space (TPF = 1 and FPR = 0), the greater the discriminant capacity [45].

Table 2. General structure of the confusion matrix developed according to the application of PLS-DA.

		Predicted	
		POS	**NEG**
Actual	POS	TP (true positive)	FN (false negative)
	NEG	FP (false positive)	TN (true negative)

POS: positive classification corresponding to a value of 1; NEG: negative classification corresponding to a value of 0.

The dataset was divided into the training and test sets using a duplex algorithm [46], so 70% was used in the development of the classification model, while the remaining 30% was used for the validation of the model. The statistics of the best model were recorded using the R^2p (determination coefficient of prediction), RMSEP (root mean square error of prediction), RER (range to error ratio) and RPD (ratio of prediction deviation). These values permitted us to define the applicative degree of the model. As stated by different authors [47–49], RER should be between 7 and 20 for quality screening, and above 20 for quality control applications, while RPD should be above 3 for screening use and above 5 for control applications. All the computations were performed in MATLAB (ver. 7.10.0, The MathWorks, Natick, MA, USA) using iN–House functions based on existing algorithms.

3. Results and Discussion

3.1. Spectra (PCA)

A prior spectral analysis was performed to detect the differences in the spectral responses the between samples at each process step (according to the definitions of GR0, IN and GR1). To provide a better visualization, the entire spectral range (4000–10,000 cm^{-1}) was cut at 7500 cm^{-1} due to the presence of noise in the last part. As shown in Figure 1, the IN spectra revealed higher scattering related to the cylindrical shape, which led to the greater interference of light. The GR0 and GR1 spectra revealed homogeneous and grouped spectra, due to the dry and ground physical conditions. Furthermore, little spectral differences could be detected between 5000 and 5200 cm^{-1}, where the O–H bonds, related to water content, were concentrated. This assumption supported the use of NIR to detect the relationship between physical and chemical characteristics [53], explaining the slightly higher moisture content in the IN samples than in the ground ones due to moistening before pelletization. No evident differences between the spectra were detected between the V and T groups.

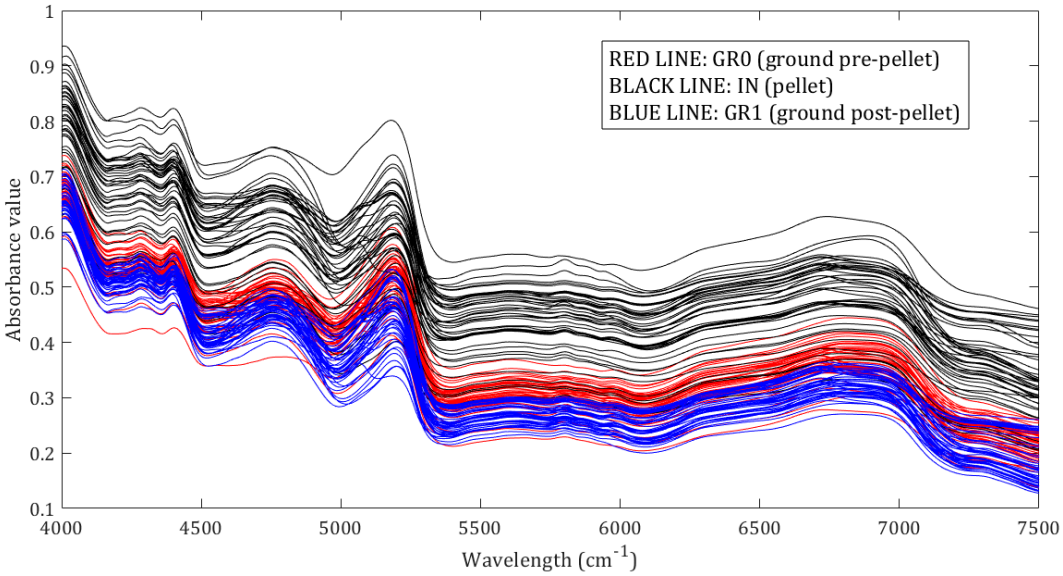

Figure 1. Averaged spectra colored according to the different processes: red lines have been used to express the GR0 spectra, black lines for the IN spectra and blue lines for the GR1 spectra.

PCA was carried out to investigate the separation between V and T according to the spectral data. The spectra were pretreated to remove scattering effects and to enhance the useful information. Two different separations were considered according to (i) the physical conditions (GR0, IN and GR1) and (ii) the classification of the origin (V and T); for both, the spectral range was cut at 7500 cm^{-1}. The results of the separation according to the physical condition are presented in the score plot (Figure 2) and the loading plot (Figure 3). The best model was developed only with the average of the spectral replicates. In fact, the first principal component (PC) explained the highest variance (97.10%) related to the main physical difference between the IN and GR groups, and the consequent interaction between the light source and the cylindrical shape of the pellets, which could favor the penetration of external light during the NIR analysis. The second PC only explained a limited residual part (1.28%) that could be related to the chemical differences of the samples (wood components and the presence of glue). Nevertheless, the chemical separation was almost completely hidden by the physical features.

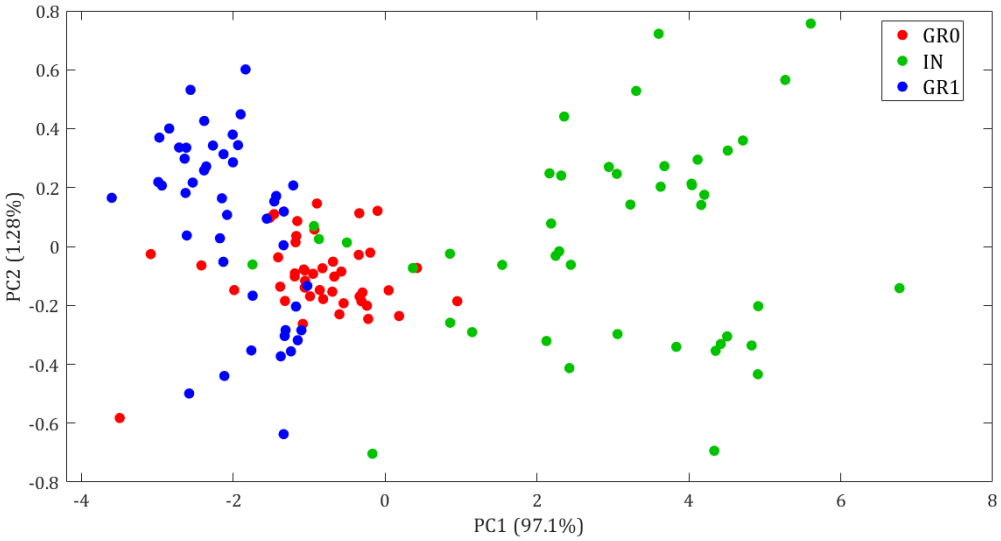

Figure 2. Score plot of the first and the second principal components (PCs) that explained the 97.1% and 1.28% of the variance, respectively. Spectra were averaged before the PCA computation.

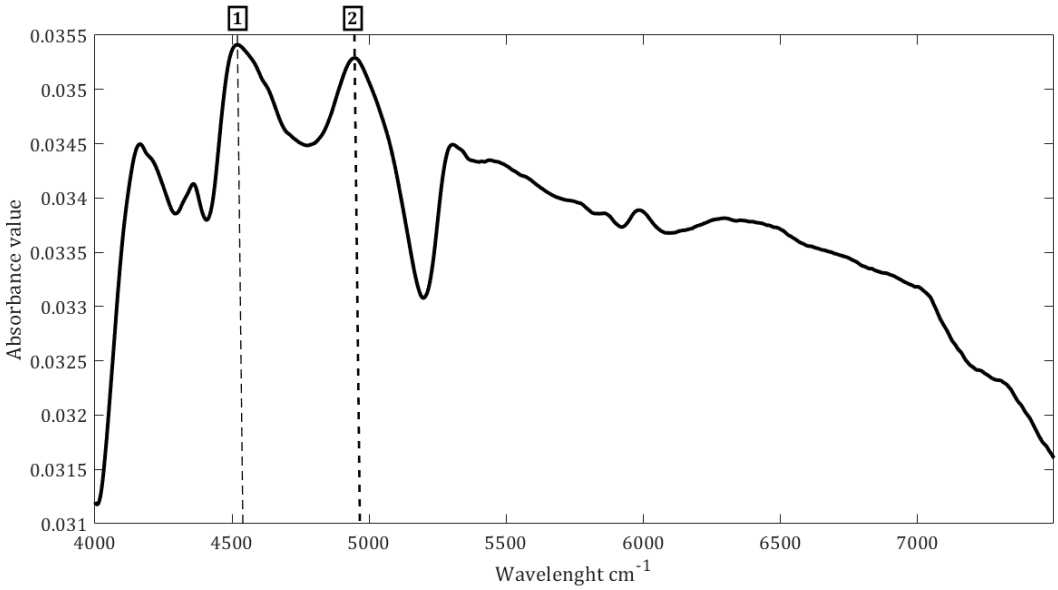

Figure 3. Loading plot of the first PC. PC2 was not considered because of the low additional variance explained. The most important discriminative wavenumbers for discrimination of the physical condition are labelled with numbers in the boxes and indicated with dashed lines.

The positive peaks detected in Figure 3 suggested that the separation may be related to the main wood components. Specifically, the peak at 4520 cm^{-1} (1) and the peak at 4952 cm^{-1} (2) are both associated with holocellulose, specifically to the C–H bonds [49,54]. As mentioned previously and confirmed by the few and broad peaks detected, the interference of light was probably involved in the increase in noise due to the scattering effect related to the physical shape of the intact pellets (IN), but this could be considered to be the only source of separation from the ground pellets (GR).

The PCA results based on the separation of V and T are presented in a score plot (Figure 4) and a loading plot (Figure 5). The best PCA model was developed by pretreating the spectra with the first derivative (Savitzky–Golay filter, second-order polynomial, 21 smoothing points) after averaging of the spectral replicates. The sum of the two PCs explained 85% of the dataset's variance, related to the main wood components and to the presence of a glue additive (industrially treated wood). Specifically, the T group spread along the positive and negative PC1 and positive PC2, while the V group mainly grouped in the negative PC1, except for the presence of few samples in the positive PC1 and negative PC2. The visual formation of little groups inside V and T are most likely related to the separation between softwood and hardwood (V), and to the degree of treatment and the amount of additives present (T).

In this separation, different components could be involved, as shown in Figure 5. The peak at 4532 cm^{-1} of PC1 (1) is probably the same shared with the peak at 4528 cm^{-1} of PC2 (5) and associated with the C–H stretching bond and C=O bonds [55]. A spectral shift also occurred for the peak at 4768 cm^{-1} of PC1 (2) and the peak at 4752 cm^{-1} of PC2 (6), both of which are associated with cellulose, and thus to C–H and O–H deformation and to O–H stretching vibrations [56]. Lastly, the peak at 4916 cm^{-1} (3) and the one at 5196 cm^{-1} (4), both for PC1, are associated with C–H deformation and the O–H stretching of lignin and cellulose, and water (O–H bonds), respectively [49,57]. In PC2, the peak at 5068 cm^{-1} (7) is associated with water, and thus with O–H stretching and deformation bonds [56]. Water's presence was confirmed as one of the main discriminative parameters due to the relevant difference between the ground material, considered to be dry, and the IN samples, where the addition of water (up to about 12%) permitted cohesion of the fine particles during the pelletization process. This result also corroborated the IN spectral peak around 5000 cm^{-1}, as shown in Figure 1.

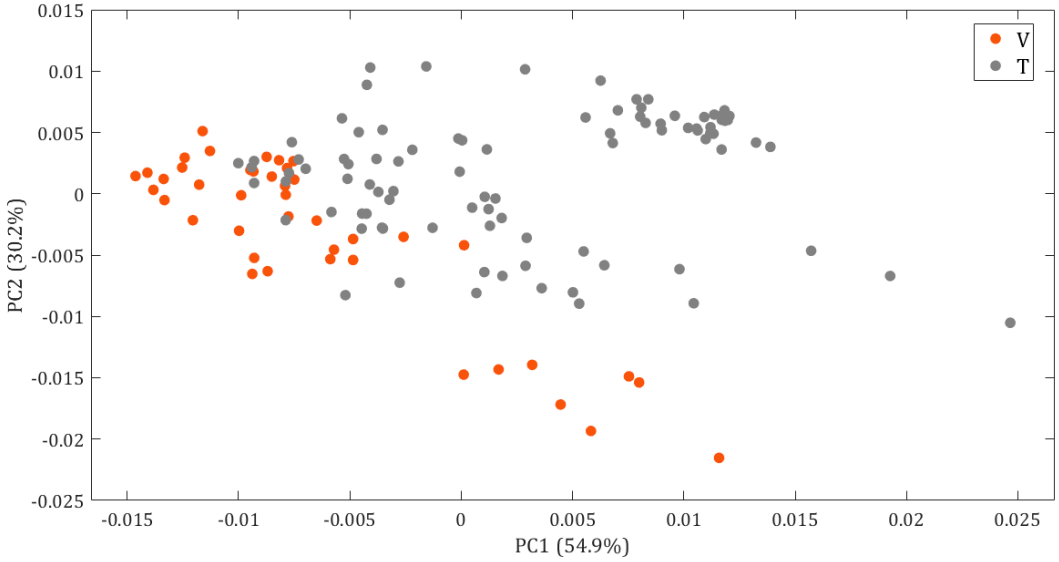

Figure 4. Score plot of the first and the second principal components (PCs) that explain 54.9% and 30.2% of the variance, respectively. Spectra have been averaged, and first derivatives (Savitzky–Golay second-order polynomial and 21 smoothing points) have been applied as spectral pretreatments.

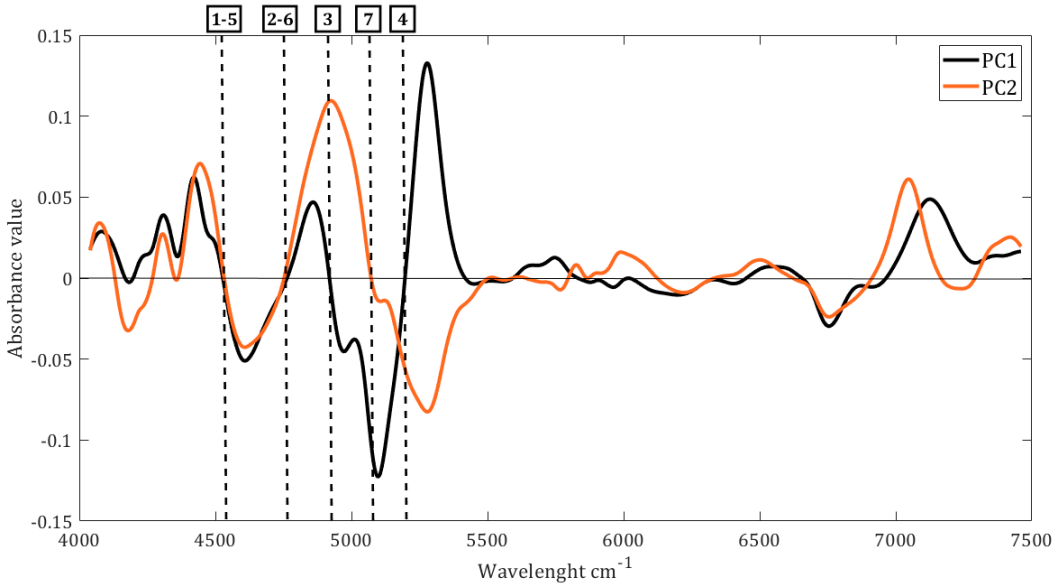

Figure 5. Loading plot of the first and second PCs. The most important discriminative wavenumbers for discrimination of the physical condition are labelled with numbers in the boxes and indicated with dashed lines. According to the spectral pretreatment considered, the positive peaks correspond to the inflection points at the intersection with the zero line.

3.2. Classification Models (PLS-DA)

The results of the classification method of PLS-DA are presented in Table 3. The computation was developed for each processing stage of the samples, including grinding and pelletization. As for the PCA methods, different spectra pretreatments were developed, based on the average of the spectral replicates to remove potential noise and scattering effects, and to enhance the useful information. Confirming the PCA computation, the spectral range (4000–10,000 cm^{-1}) was cut at 7500 cm^{-1} due to the presence of evident noise in the last part.

Table 3. Results of the classification model for each processing step. Only the performance of validation has been shown.

	GR0 (p)	IN (p)	GR1 (p)
Pretreatment	**Mean SNV**	**Mean 9der1**	**Mean 21der2**
R^2	0.82	0.37	0.70
RMSEP	0.25	0.35	0.29
ROC	0.5780	0.5440	0.6240
Sensitivity TP/(TP + FN)	1.00	1.00	1.00
Specificity TN/(TN + FP)	1.00	1.00	1.00
Accuracy	1.00	1.00	1.00
Error	0.00	0.00	0.00
Precision	1.00	1.00	1.00
Misclassification	0	0	0

GR0: ground pellet before pelletization; GR1: ground pellet after pelletization; IN: intact pellet; T: chemically treated wood; V: virgin or untreated wood; R^2: determination coefficient; RMSEP: root mean square error of prediction.

Although the same highest value of accuracy was obtained for each classification model at each step (accuracy = 1 and misclassification = 0), the best one was with the GR0 dataset according to the model's results and the error. The spectra were pretreated with SNV after averaging of the spectral replicates. The lower performance of IN models was related to the higher scattering effect due to the cylindrical shape of the intact pellets, which facilitated the formation of random holes during the placement of the sample in the spectrophotometer's cup. The physical condition of ground pellets led to a more homogeneous distribution, avoiding the interference of external light. Moreover, Figure 6a,b shows the score plot and the regression vector plot of the GR0 model. The PC1 mostly explained the dataset's variability, related to the degree of industrial treatment. The samples' distribution revealed a net separation between virgin wood, which was more homogenous, and the treated group, which varied along PC1. Furthermore, test samples were correctly classified following the distribution of each group, confirming the model's results. One virgin sample (oak) was detected and removed as an outlier, while the mixed softwood sample was placed close to the treated group, confirming the chemical differences between hardwood and softwood and the use of residual fir in the wood industry [33,54]. The main peaks detected in the regression vector plot (Figure 6b) revealed that the wood component and the influence of water were involved in the separation. Specifically, the peak at 4328 cm^{-1} of PC1 (1) is associated with the C–H bonds of holocellulose [49], and the peak at 5776 cm^{-1} (3) is related to cellulose and associated with the first overtone of the C–H stretching bonds. Nevertheless, the difficulties of interpretation in the range of 5000–4000 cm^{-1} could lead to improper identification of the components [56] but could be related to N–H vibrations associated with formaldehyde [58]. The effect of water is related to the peak at 5144 cm^{-1} (2), and thus to the stretching and deformation of O–H bonds [55], despite it being less evident due to the dry condition of the GR samples.

According to the GR1 and IN classification models, lower classification performances were obtained for the IN dataset, due to the higher spectral noise. Averaged spectra replicates of GR1 were pretreated with second derivatives (Savitzky–Golay filter, second-order polynomial, 21 smoothing points). Figure 7a,b shows the score plot and the regression vector plot of the GR1 model. PC1 explained 53.35% of the variance, followed by 23.43% explained by PC2. The samples' distribution revealed an unclear separation between virgin wood, located in the negative PC1 but also the positive PC2, and treated group, which showed the formation of smaller groups of samples, probably related to different degrees of industrial treatment. The test samples also showed a similar distribution, confirming the good performance of the model and its classification accuracy, which was similar to that of GR0. For this reason, no outliers could be clearly detected. The main peaks detected in the regression vector plot (Figure 7b) revealed the influence of the main wood components but also of the water at 5056 cm^{-1} (7), associated with O–H stretching and deformation [56],

while the peak at 5908 cm^{-1} (8) is related to the first overtone of C–H bonds, probably associated with lignin [55]. The peak at 4076 cm^{-1} (1) is associated with the C–H and C-C bonds of carbohydrates [56], while the peak at 4152 cm^{-1} (2) and at 4872 cm^{-1} (6) is related to cellulose, and thus to O–H and C–H stretching and deformation bonds [54]. The peak at 4352 cm^{-1} (3) is associated with C-O, C–H_2 and also O–H vibrational bonds [57]. The peaks detected at 4436 cm^{-1} (4) and 4616 cm^{-1} (5) were noteworthy, probably related to the presence of glue; therefore, they are associated with N–H and C–H_2 bonds, confirming the presence of industrially treated material [49].

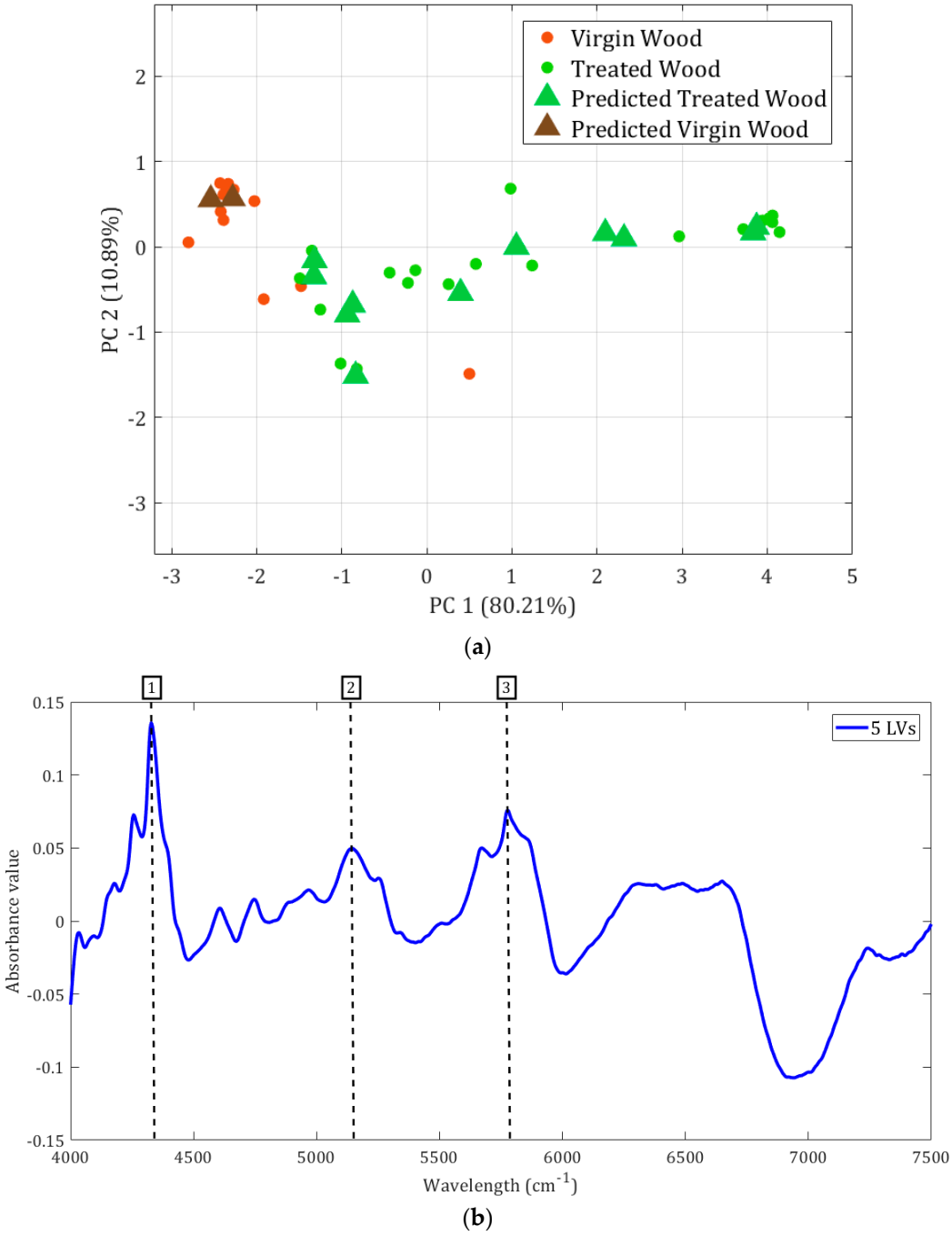

Figure 6. Results of the GR0 model and pretreating the spectra with SNV: (**a**) the score plot of the first and second PCs, and (**b**) the regression vector plot using five latent variables. The most important discriminative positive peaks are labelled with numbers in the boxes and indicated with dashed lines.

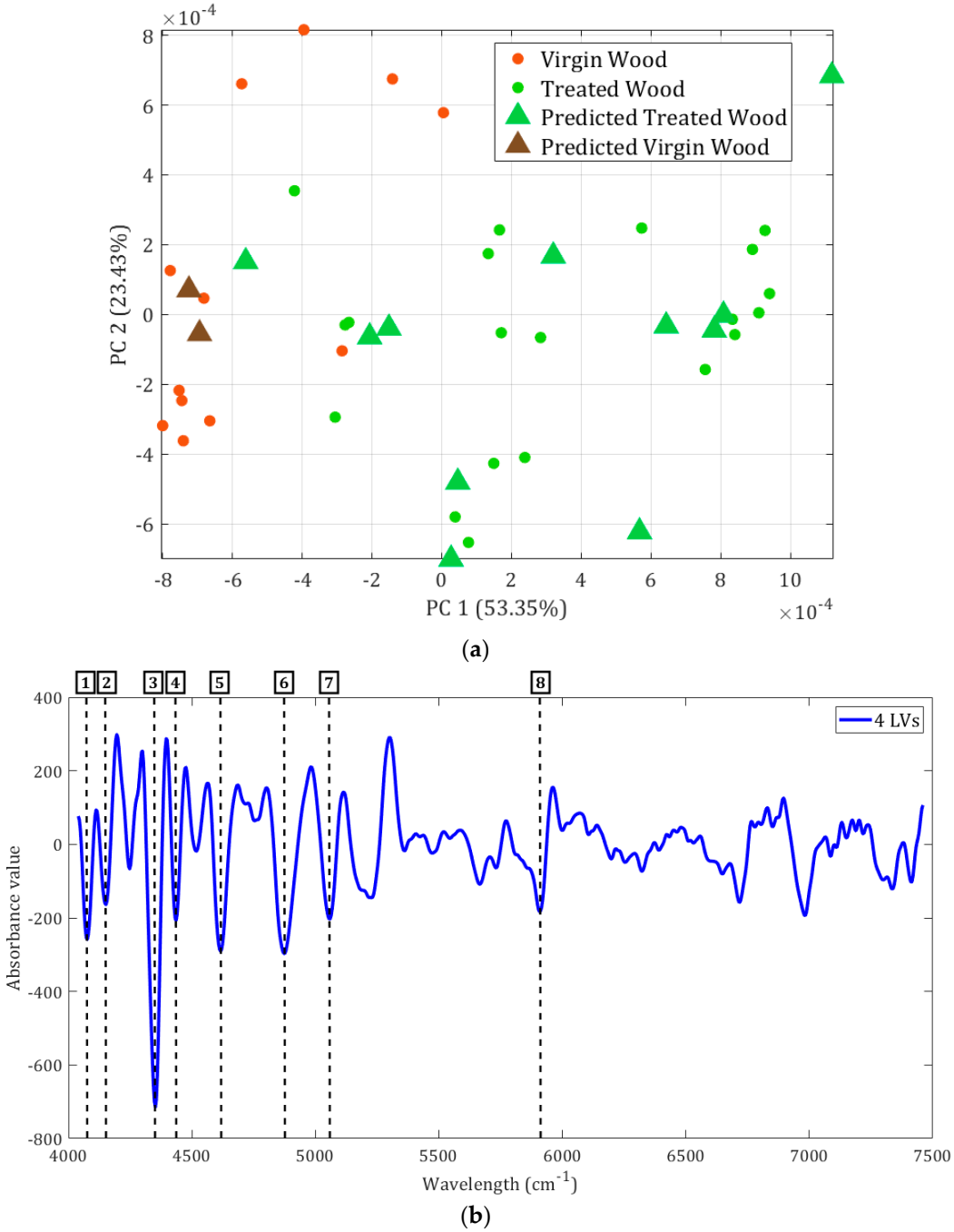

Figure 7. Results for the GR1 model and pretreating the spectra with second derivatives (Savitzky–Golay filter, second-order polynomial, 21 smoothing points): (**a**) score plot of the first and second PCs, and (**b**) the regression vector plot using five latent variables. The most important discriminative negative peaks are labelled with numbers in the boxes and indicated with dashed lines.

The best IN model was developed with the first derivative (Savitzky–Golay filter, second-order polynomial, nine smoothing points) after averaging of the spectral replicates. Figure 8a,b shows the score plot and the regression vector plot of the IN model, where, as for the GR1 model, PC1 explained almost half of the variance (54.42%), followed by the remaining 37.43% being explained by PC2. The samples' distribution revealed that both groups varied along PC2, despite their scattered positioning, but treated group also varied along PC1, which confirmed the creation of smaller sub-groups. The test samples led to a similar distribution to the training set, confirming the good validation results

despite the lower performance with the lower R^2 and the higher error. Extreme virgin samples could be detected and were considered as outliers. The main peaks detected in the regression vector plot (Figure 8b) are mostly related to lignin, cellulose and water. Specifically, the peaks at 4144 cm^{-1} (1), at 4520 cm^{-1} (3) and at 4760 cm^{-1} (4) are related to cellulose and holocellulose, associated with C–H, O–H and C=O stretching and bending vibrations [54–56]. Great importance is related to the detection of lignin at the peak at 5980 cm^{-1} (7) and 6920 cm^{-1} (8), respectively, associated with the first overtone of the stretching of the carbonyl group [56] and with the C–H vibrational bonds, and also with the first overtone of O–H bonds [55], confirming the relevance of lignin in the intact pellets. Furthermore, water was also clearly detected at 5044 (5) and 5212 cm^{-1} (6) due to the O–H stretching and deformation bonds [54,56]. Lastly, the peak at 4336 cm^{-1} (2) could be compared with the peaks detected at 4328 cm^{-1} in the GR0 model, so they are presumably related to formaldehyde's presence due to the N–H bonds associated with NIR detection in that range [58].

Summarizing the results, the spectral peaks detected in the interval of lignin's wavelengths highlight the effect of the thermo-chemical transformation occurring during pelletization. Namely, the meltdown of lignin improved its natural "adhesive" function [59] and, in fact, it was mainly detected in the IN samples. Nevertheless, the relevant difference between ground and intact pellets related to their physical condition could conceal spectral information about the chemical features. Thus, specific chemical investigations could be necessary to further explore the alteration of lignin in terms of the concentration and/or modification. Moreover, the cylindrical shape of the pellets could facilitate the presence of gaps, thus leading to negative interactions with light during the NIR analysis; therefore, additional devices to avoid the influence of external variations should be considered. Furthermore, the proposed models only identified the presence of glue and did not provide any information about the presence of other materials such as plastics or inert components. Further tests using specific plastic constituents and non-woody elements could support the development of more elaborate models, leading to a wider investigation.

The process of pelletization implies high temperatures and pressures, leading to thermo-chemical reactions that could lead to unusual reactions of the chemical components in non-virgin materials. Therefore, compared with the spectral response of glue in the GR0 samples, the glue portion in GR1 could be potentially highlighted by the loss of O–H bonds produced by the heating during pelletization, allowing for clearer detection of the N–H bonds. Instead, the reduced evidence of glue bonds in IN could be covered by the noise produced by the scattering effect, confirming by the spectral peaks and the lower classification performance.

Lastly, expanding the dataset by increasing the number of analyzed samples could support the development of more reliable classification models and provide robust information about the main chemical features.

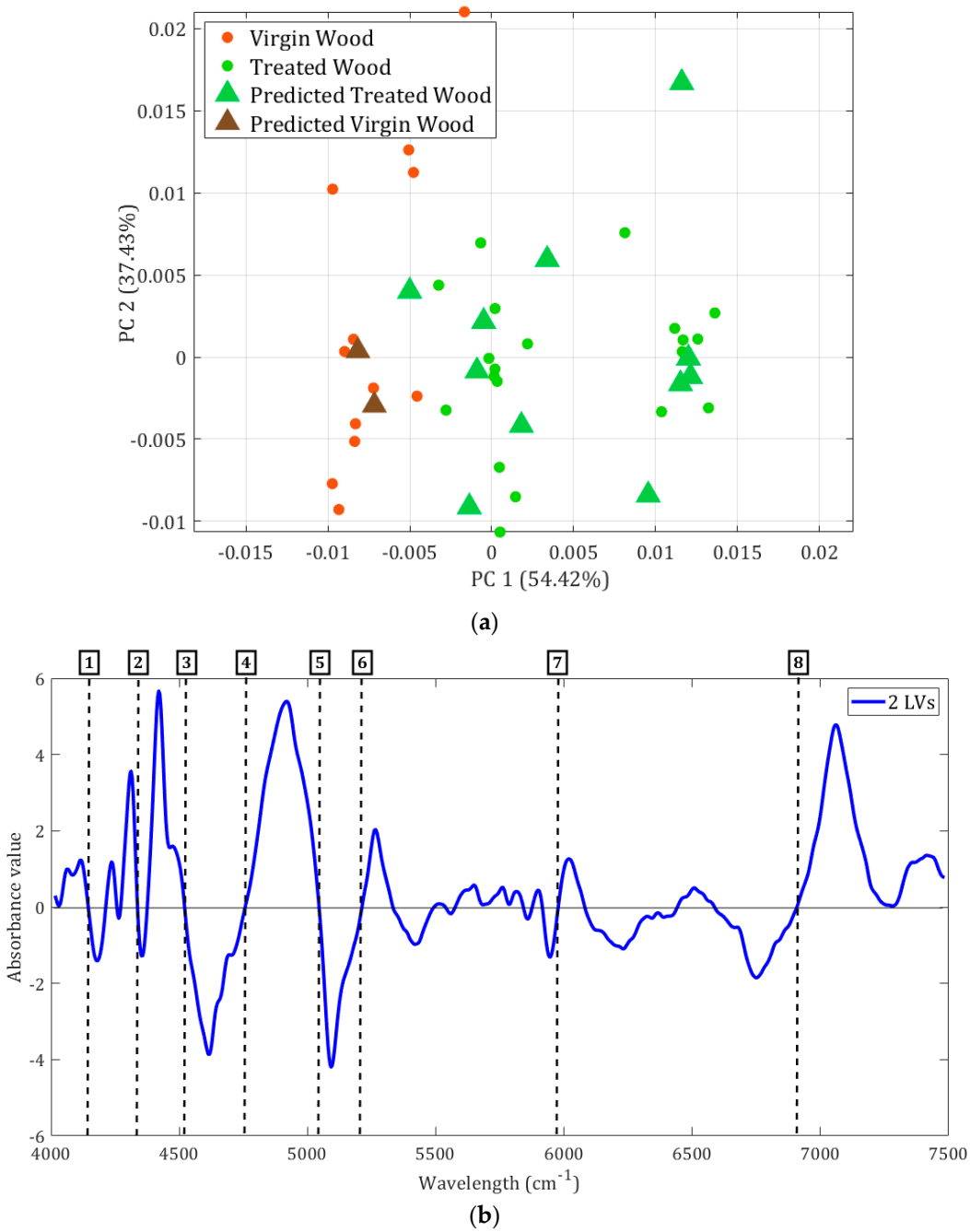

Figure 8. Results of the IN model and pretreating the spectra with first derivatives (Savitzky–Golay filter, second-order polynomial, nine smoothing points): (**a**) score plot of the first and second PCs, and (**b**) the regression vector plot using five latent variables. The most important discriminative peaks, in the inflection points at the intersection with the zero line, are labelled with numbers in the boxes and indicated with dashed lines.

4. Conclusions

The separation between virgin and treated wood is a crucial step in monitoring the quality of densified biofuels, such as pellets. The physical compactness and homogeneity of densified materials leads to the impossibility of identifying the source materials, facilitating the illegal addition of waste and environmentally harmful materials, such as glue-treated wood. Near infrared spectroscopy (NIR) could be considered a valid alternative to standard analyses for the qualitative assessment of solid biofuels, being time-efficient, non-destructive, and cost-effective. Furthermore, the application of chemometrics and

classification methods (PLS-DA) could support NIR analyses in determination of the origin of woody components, allowing the detection of fraudulent biofuels.

Thus, as shown through this study, discrimination between virgin and chemically treated pellet appears to be feasible, both in intact and ground pellets, despite the lower performance detected for the non-ground pellets due to the higher scattering effect. Water bonds, cellulose and lignin are mainly responsible for the identification of the two groups, while glue bonds were detected in specific conditions due to the potential effect of thermo-chemical processes occurring during pelletization, which might lead to the alteration of woody and non-woody components. Lignin, in particular, can act as an adhesive under high temperatures and pressures, confirming its influence in the process of pelletization.

According to the current results, the alternative method of NIR can be considered a reliable tool for real-time applications and continuous monitoring. Although its usability could improve with the help of portable instruments, benchtop spectrophotometer can simulate an in-line approach, resulting in higher representativeness of the analysis according to the larger testing spot and the large number of scans. Implementing NIR in in-line systems can also facilitate the detection of irregularities directly in power plants, thereby enhancing the production of quality products and the overall quality of the market.

Author Contributions: Conceptualization, E.L. and T.G.; methodology, E.L. and T.G.; software, E.L.; validation, E.L., T.G. and D.D.; formal analysis, E.L. and T.G.; investigation, E.L., T.G., N.D.M. and R.P.; resources, E.L., T.G. and R.P.; data curation, E.L. and N.D.M.; writing—original draft preparation, T.G.; writing—review and editing, E.L., T.G. and D.D.; visualization, E.L., T.G. and D.D.; supervision, G.T. and R.P.; project administration, E.L. and G.T.; funding acquisition, G.T. All authors have read and agreed to the published version of the manuscript.

Funding: This research received no external funding.

Data Availability Statement: The data presented in this study are available on request from the corresponding author.

Acknowledgments: Progetto ECS 0000024 Rome Technopole—CUP B83C22002820006, PNRR Missione 4 Componente 2 Investimento 1.5, Finanziato dall'Unione Europea—NextGenerationEU.

Conflicts of Interest: The authors declare no conflict of interest.

References

1. Glavonjić, B.D.; Krajnc, N.; Palus, H. Development of Wood Pellets Market in South East Europe. *Therm. Sci.* **2015**, *19*, 781–792. [CrossRef]
2. Proskurina, S.; Alakangas, E.; Heinimö, J.; Mikkilä, M.; Vakkilainen, E. A Survey Analysis of the Wood Pellet Industry in Finland: Future Perspectives. *Energy* **2017**, *118*, 692–704. [CrossRef]
3. Schipfer, F.; Kranzl, L.; Olsson, O.; Lamers, P. The European Wood Pellets for Heating Market-Price Developments, Trade and Market Efficiency. *Energy* **2020**, *212*, 118636. [CrossRef]
4. Eurostat Data Browser-Roundwood, Fuelwood and Other Basic Products. Available online: https://ec.europa.eu/eurostat/databrowser/ (accessed on 31 October 2023).
5. European Commission. *Communication from the Commission to the European Parliament, the European Council, the Council, the European Economic and Social Committee and the Committee of Regions*; A Green Deal Industrial Plan for the Net-Zero, Age; COM (2023) 62, ch II; European Commission: Luxembourg, 2023.
6. Johansson, L.S.; Leckner, B.; Gustavsson, L.; Cooper, D.; Tullin, C.; Potter, A. Emission Characteristics of Modern and Old-Type Residential Boilers Fired with Wood Logs and Wood Pellets. *Atmos. Environ.* **2004**, *38*, 4183–4195. [CrossRef]
7. Ozgen, S.; Caserini, S.; Galante, S.; Giugliano, M.; Angelino, E.; Marongiu, A.; Hugony, F.; Migliavacca, G.; Morreale, C. Emission Factors from Small Scale Appliances Burning Wood and Pellets. *Atmos. Environ.* **2014**, *94*, 144–153. [CrossRef]
8. Dahal, K.; Tissari, J.; Hartmann, H.; Schön, C.; Fraboulet, I.; Cea, B.; Kubesa, P.; Horak, J. *Technical Report on Review of Particulate Emissions Produced from the Small-Scale Solid Fuel Combustion*; University of Eastern Finland: Kuopio, Finland, 2022. [CrossRef]
9. Bäfver, L.S.; Leckner, B.; Tullin, C.; Berntsen, M. Particle Emissions from Pellets Stoves and Modern and Old-Type Wood Stoves. *Biomass Bioenergy* **2011**, *35*, 3648–3655. [CrossRef]
10. Toscano, G.; Duca, D.; Amato, A.; Pizzi, A. Emission from Realistic Utilization of Wood Pellet Stove. *Energy* **2014**, *68*, 644–650. [CrossRef]
11. Arranz, J.I.; Miranda, M.T.; Montero, I.; Sepúlveda, F.J.; Rojas, C.V. Characterization and Combustion Behaviour of Commercial and Experimental Wood Pellets in South West Europe. *Fuel* **2015**, *142*, 199–207. [CrossRef]

12. Stubenberger, G.; Scharler, R.; Zahirović, S.; Obernberger, I. Experimental Investigation of Nitrogen Species Release from Different Solid Biomass Fuels as a Basis for Release Models. *Fuel* **2008**, *87*, 793–806. [CrossRef]
13. Garcia-Maraver, A.; Zamorano, M.; Fernandes, U.; Rabaçal, M.; Costa, M. Relationship between Fuel Quality and Gaseous and Particulate Matter Emissions in a Domestic Pellet-Fired Boiler. *Fuel* **2014**, *119*, 141–152. [CrossRef]
14. Mack, R.; Schön, C.; Kuptz, D.; Hartmann, H.; Brunner, T.; Obernberger, I.; Behr, H.M. Influence of Pellet Length, Content of Fines, and Moisture Content on Emission Behavior of Wood Pellets in a Residential Pellet Stove and Pellet Boiler. *Biomass Convers. Biorefinery* **2022**, *1*, 1–18. [CrossRef]
15. Wöhler, M.; Jaeger, D.; Reichert, G.; Schmidl, C.; Pelz, S.K. Influence of Pellet Length on Performance of Pellet Room Heaters under Real Life Operation Conditions. *Renew. Energy* **2017**, *105*, 66–75. [CrossRef]
16. Thunman, H.; Leckner, B. Influence of Size and Density of Fuel on Combustion in a Packed Bed. *Proc. Combust. Inst.* **2005**, *30*, 2939–2946. [CrossRef]
17. Mack, R.; Schön, C.; Kuptz, D.; Hartmann, H.; Brunner, T.; Obernberger, I.; Behr, H.M. Influence of Wood Species and Additives on Emission Behavior of Wood Pellets in a Residential Pellet Stove and a Boiler. *Biomass Convers. Biorefinery* **2023**, *1*, 1–20. [CrossRef]
18. *ISO 17225-2:2021*; Solid Biofuels—Fuel Specifications and Classes—Part 2: Graded Wood Pellets. ISO: Geneva, Switzerland, 2021.
19. Risholm-Sundman, M.; Vestin, E. Emissions during Combustion of Particleboard and Glued Veneer. *Eur. J. Wood Wood Prod.* **2005**, *63*, 179–185. [CrossRef]
20. Jiang, J.; Luo, J.; Wu, Y.; Qu, W. The Influence of Ammonium Polyphosphate on the Smoke Toxicity of Wood Materials. *Thermochim. Acta* **2023**, *725*, 179534. [CrossRef]
21. Hagel, S.; Saake, B. Fractionation of Waste MDF by Steam Refining. *Molecules* **2020**, *25*, 2165. [CrossRef]
22. Szczurek, A.; Maciejewska, M.; Zajiczek, Ż.; Mościcki, K. Detection of Emissions from the Combustion of Wood-Based Materials Being Furniture Industry Waste. *Atmos. Pollut. Res.* **2021**, *12*, 375–385. [CrossRef]
23. *Ministero Dell'Ambiente e Della Tutela Del Territorio e Del Mare*; Italian Ministerial Decree November 2017, n. 186.; Gazzetta Ufficiale: Rome, Italy, 2017.
24. Regione Marche. *Allegato-A. Misure Contingenti 2021/2022 Per La Riduzione Della Concentrazione Degli Inquinanti In Aria Ambiente Nel Territorio Dei Comuni Della Zona Costiera E Valliva*; Deliberazione Della Giunta Regionale; Decision of the regional government 2021/2022; Regione Marche: Ancona, Italy, 2022.
25. Gillespie, G.D.; Everard, C.D.; McDonnell, K.P. Prediction of Biomass Pellet Quality Indices Using near Infrared Spectroscopy. *Energy* **2015**, *80*, 582–588. [CrossRef]
26. Sánchez-Gatón, M.Á.; Campos, M.I.; Segovia, J.J. Prediction for Total Moisture Content in Wood Pellets by near Infrared Spectroscopy (NIRS). *Dyna* **2021**, *93*, 296–301. [CrossRef] [PubMed]
27. Posom, J.; Shrestha, A.; Saechua, W.; Sirisomboon, P. Rapid Non-Destructive Evaluation of Moisture Content and Higher Heating Value of Leucaena Leucocephala Pellets Using near Infrared Spectroscopy. *Energy* **2016**, *107*, 464–472. [CrossRef]
28. Zhu, M.Z.; Wen, B.; Wu, H.; Li, J.; Lin, H.; Li, Q.; Li, Y.; Huang, J.; Liu, Z. The Quality Control of Tea by Near-Infrared Reflectance (NIR) Spectroscopy and Chemometrics. *J. Spectrosc.* **2019**, *2019*, 8129648. [CrossRef]
29. Segelke, T.; Schelm, S.; Ahlers, C.; Fischer, M. Food Authentication: Truffle (*Tuber* Spp.) Species Differentiation by FT-NIR and Chemometrics. *Foods* **2020**, *9*, 922. [CrossRef]
30. Wold, S.; Sjöström, M.; Eriksson, L. PLS-Regression: A Basic Tool of Chemometrics. *Chemom. Intell. Lab. Syst.* **2001**, *58*, 109–130. [CrossRef]
31. Stocchero, M.; De Nardi, M.; Scarpa, B. PLS for Classification. *Chemom. Intell. Lab. Syst.* **2021**, *216*, 104374. [CrossRef]
32. Brandily, M.L.; Monbet, V.; Bureau, B.; Boussard-Plédel, C.; Loréal, O.; Adam, J.L.; Sire, O. Identification of Foodborne Pathogens within Food Matrices by IR Spectroscopy. *Sens. Actuators B. Chem.* **2011**, *160*, 202–206. [CrossRef]
33. Duca, D.; Mancini, M.; Rossini, G.; Mengarelli, C.; Foppa Pedretti, E.; Toscano, G.; Pizzi, A. Soft Independent Modelling of Class Analogy Applied to Infrared Spectroscopy for Rapid Discrimination between Hardwood and Softwood. *Energy* **2016**, *117*, 251–258. [CrossRef]
34. Duca, D.; Pizzi, A.; Mancini, M.; Rossini, G.; Mengarelli, C.; Ilari, A.; Lucesoli, G.; Toscano, G.; Foppa Pedretti, E. Fast Measurement by Infrared Spectroscopy as Support to Woody Biofuels Quality Determination. *J. Agric. Eng.* **2016**, *47*, 17–21. [CrossRef]
35. Sandak, J.; Sandak, A.; Zitek, A.; Hintestoisser, B.; Picchi, G. Development of Low-Cost Portable Spectrometers for Detection of Wood Defects. *Sensors* **2020**, *20*, 545. [CrossRef]
36. Lixourgioti, P.; Goggin, K.A.; Zhao, X.; Murphy, D.J.; van Ruth, S.; Koidis, A. Authentication of Cinnamon Spice Samples Using FT-IR Spectroscopy and Chemometric Classification. *LWT* **2022**, *154*, 112760. [CrossRef]
37. Dupuy, N.; Galtier, O.; Ollivier, D.; Vanloot, P.; Artaud, J. Comparison between NIR, MIR, Concatenated NIR and MIR Analysis and Hierarchical PLS Model. Application to Virgin Olive Oil Analysis. *Anal. Chim. Acta* **2010**, *666*, 23–31. [CrossRef] [PubMed]
38. Correia, R.M.; Tosato, F.; Domingos, E.; Rodrigues, R.R.T.; Aquino, L.F.M.; Filgueiras, P.R.; Lacerda, V.; Romão, W. Portable near Infrared Spectroscopy Applied to Quality Control of Brazilian Coffee. *Talanta* **2018**, *176*, 59–68. [CrossRef] [PubMed]
39. Park, S.Y.; Kim, J.C.; Kim, J.H.; Yang, S.Y.; Kwon, O.; Yeo, H.; Cho, K.C.; Choi, I.G. Possibility of Wood Classification in Korean Softwood Species Using Near-Infrared Spectroscopy Based on Their Chemical Compositions. *J. Korean Wood Sci. Technol.* **2017**, *45*, 202–212. [CrossRef]
40. Cooper, P.A.; Jeremic, D.; Radivojevic, S.; Ung, Y.T.; Leblon, B. Potential of Near-Infrared Spectroscopy to Characterize Wood Products 1. *Can. J. For. Res.* **2011**, *41*, 2150–2157. [CrossRef]

41. Duca, D.; Pizzi, A.; Rossini, G.; Mengarelli, C.; Foppa Pedretti, E.; Mancini, M. Prediction of Hardwood and Softwood Contents in Blends of Wood Powders Using Mid-Infrared Spectroscopy. *Energy Fuels* **2016**, *30*, 3038–3044. [CrossRef]
42. Measurement of CO Concentration in Combustion Field Based on Mid-Infrared Absorption Spectroscopy-Web of Science Core Collection. Available online: https://www.webofscience.com (accessed on 2 November 2023).
43. Nascimbem, L.B.L.R.; Rubini, B.R.; Poppi, R.J. Determination of Quality Parameters in Moist Wood Chips by Near Infrared Spectroscopy Combining PLS-DA and Support Vector Machines. *J. Wood Chem. Technol.* **2013**, *33*, 247–257. [CrossRef]
44. Pfautsch, S.; Macfarlane, C.; Ebdon, N.; Meder, R. Assessing Sapwood Depth and Wood Properties in Eucalyptus and Corymbia Spp. Using Visual Methods and near Infrared Spectroscopy (NIR). *Trees-Struct. Funct.* **2012**, *26*, 963–974. [CrossRef]
45. Braga, J.W.B.; Pastore, T.C.M.; Coradin, V.T.R.; Camargos, J.A.A.; Da Silva, A.R. The Use of near Infrared Spectroscopy to Identify Solid Wood Specimens of Swietenia Macrophylla (Cites Appendix II). In *Proceedings of the IAWA Journal*; Brill Academic Publishers: Leiden, The Netherlands, 2011; Volume 32, pp. 285–296.
46. Espinoza, J.A.; Hodge, G.R.; Dvorak, W.S. The Potential Use of near Infrared Spectroscopy to Discriminate between Different Pine Species and Their Hybrids. *J. Near Infrared Spectrosc.* **2012**, *20*, 437–447. [CrossRef]
47. Mancini, M.; Taavitsainen, V.M.; Toscano, G. Comparison of Three Different Classification Methods Performance for the Determination of Biofuel Quality by Means of NIR Spectroscopy. *J. Chemom.* **2019**, *33*, e3145. [CrossRef]
48. Mancini, M.; Rinnan; Pizzi, A.; Mengarelli, C.; Rossini, G.; Duca, D.; Toscano, G. Near Infrared Spectroscopy for the Discrimination between Different Residues of the Wood Processing Industry in the Pellet Sector. *Fuel* **2018**, *217*, 650–655. [CrossRef]
49. Mancini, M.; Rinnan, Å.; Pizzi, A.; Toscano, G. Use of Fourier Transform near Infrared Spectroscopy for the Detection of Residues from Wood Processing Industry in the Pellet Sector. *J. Chemom.* **2019**, *33*, 77–84.
50. Toscano, G.; Maceratesi, V.; Leoni, E.; Stipa, P.; Laudadio, E.; Sabbatini, S. FTIR Spectroscopy for Determination of the Raw Materials Used in Wood Pellet Production. *Fuel* **2022**, *313*, 123017. [CrossRef]
51. Rinnan, Å.; van den Berg, F.; Engelsen, S.B. Review of the Most Common Pre-Processing Techniques for near-Infrared Spectra. *TrAC-Trends Anal. Chem.* **2009**, *28*, 1201–1222. [CrossRef]
52. Pasquini, C. Near Infrared Spectroscopy: A Mature Analytical Technique with New Perspectives–A Review. *Anal. Chim. Acta* **2018**, *1026*, 8–36. [CrossRef]
53. Tsuchikawa, S.; Kobori, H. A Review of Recent Application of near Infrared Spectroscopy to Wood Science and Technology. *J. Wood Sci.* **2015**, *61*, 213–220. [CrossRef]
54. Toscano, G.; Rinnan, Å.; Pizzi, A.; Mancini, M. The Use of Near-Infrared (NIR) Spectroscopy and Principal Component Analysis (PCA) to Discriminate Bark and Wood of the Most Common Species of the Pellet Sector. *Energy Fuels* **2017**, *31*, 2814–2821. [CrossRef]
55. Fujimoto, T.; Kurata, Y.; Matsumoto, K.; Tsuchikawa, S. Feasibility of Near-Infrared Spectroscopy for Online Multiple Trait Assessment of Sawn Lumber. *J. Wood Sci.* **2010**, *56*, 452–459. [CrossRef]
56. Schwanninger, M.; Rodrigues, J.C.; Fackler, K. A Review of Band Assignments in near Infrared Spectra of Wood and Wood Components. *J. Near Infrared Spectrosc.* **2011**, *19*, 287–308. [CrossRef]
57. Sandak, J.; Sandak, A.; Pauliny, D.; Krasnoshlyk, V.; Hagman, O. Near Infrared Spectroscopy as a Tool for Estimation of Mechanical Stresses in Wood. *Adv. Mater. Res.* **2013**, *778*, 448–453. [CrossRef]
58. Minopoulou, E.; Dessipri, E.; Chryssikos, G.D.; Gionis, V.; Paipetis, A.; Panayiotou, C. Use of NIR for Structural Characterization of Urea-Formaldehyde Resins. *Int. J. Adhes. Adhes.* **2003**, *23*, 473–484. [CrossRef]
59. Watkins, D.; Nuruddin, M.; Hosur, M.; Tcherbi-Narteh, A.; Jeelani, S. Extraction and Characterization of Lignin from Different Biomass Resources. *J. Mater. Res. Technol.* **2015**, *4*, 26–32. [CrossRef]